ACS Catalysis

pubs.acs.org/acscatalysis Research Article

Cobalt-Catalyzed Coupling of Aryl Chlorides with Aryl Boron Esters Activated by Alkoxides

Sanita B. Tailor,[†] Mattia Manzotti,[†] Gavin J. Smith, Sean A. Davis, and Robin B. Bedford*

Cite This: *ACS Catal.* 2021, 11, 3856–3866 Read Online

ACCESS | Metrics & More | Article Recommendations | Supporting Information

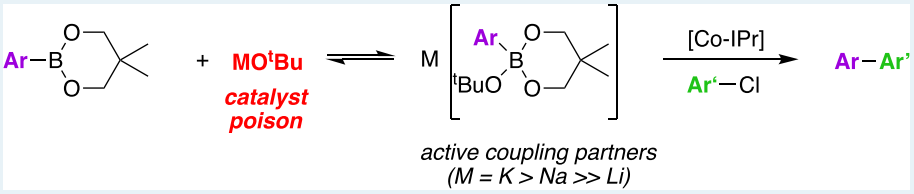

ABSTRACT: The cobalt-catalyzed Suzuki biaryl cross-coupling of aryl chloride substrates with aryl boron reagents, activated with more commonly used bases, remained a significant unmet challenge in the race to replace platinum group metal catalysts with Earth-abundant metal alternatives. We now show that this highly desirable process can be realized using alkoxide bases, provided the right counterion is employed, strict stoichiometric control of the base is maintained with respect to the aryl boron reagent, and the correct boron ester is selected. Potassium *tert*-butoxide works well, but any excess of the base first inhibits and then poisons the catalyst. Lithium *tert*-butoxide performs very poorly, while even catalytic amounts of lithium additives also poison the catalyst. Meanwhile, a neopentane diol-based boron ester is required for best performance. As well as delivering this sought-after transformation, we have undertaken detailed mechanistic and computational investigations to probe the possible mechanism of the reaction and help explain the unexpected experimental observations.

KEYWORDS: *cobalt, Suzuki, aryl chlorides, aryl boron, alkoxide*

INTRODUCTION

Biaryls are widely found in pharmaceuticals, agrochemicals, and materials, and the Suzuki biaryl coupling reaction (Figure 1) is a powerful, robust, and widely exploited method for the production of this structural motif.[1,2] By far the most widely used catalysts for the Suzuki reaction are homogeneous species based on palladium, and these have been applied to a vast range of processes, including the commercial synthesis of pharmaceutical intermediates such as *o*-tolyl benzonitrile (OTBN)—used in the production of six different sartan-class drugs for the treatment of hypertension—and in BASF's production of boscalid, a broad-spectrum fungicide.[3] Despite the unrivaled success enjoyed by palladium, its application has serious drawbacks: palladium is expensive, scarce, and its extraction is environmentally deleterious; in addition, the inherent toxicity of all platinum group metals (PGMs) means that there are stringent regulatory requirements limiting the levels of palladium that can be present in active pharmaceutical intermediates to the low-ppm range.[4] Accordingly, there is a drive to replace palladium and other PGMs with more benign alternatives based on less-toxic Earth-abundant metals (EAMs) in a range of catalytic transformations.[5]

Of the EAMs investigated as replacements for PGMs in cross-coupling reactions, those based on first-row transition metals are particularly attractive due to their relatively low cost,

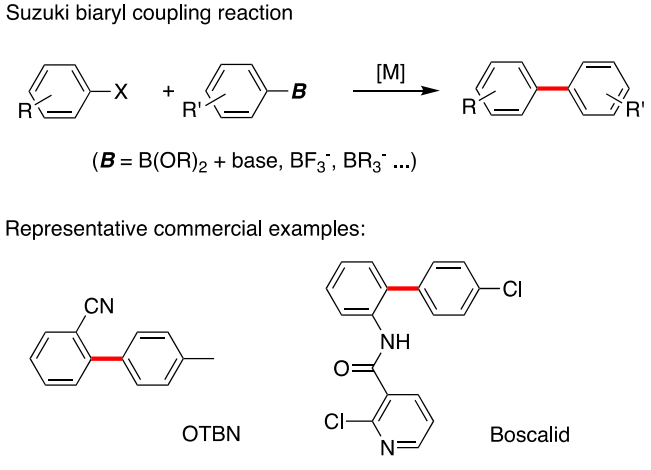

Figure 1. Suzuki biaryl cross-coupling and selected commercial examples.

Received: December 18, 2020
Revised: February 24, 2021
Published: March 12, 2021

https://dx.doi.org/10.1021/acscatal.0c05557
ACS Catal. 2021, 11, 3856–3866

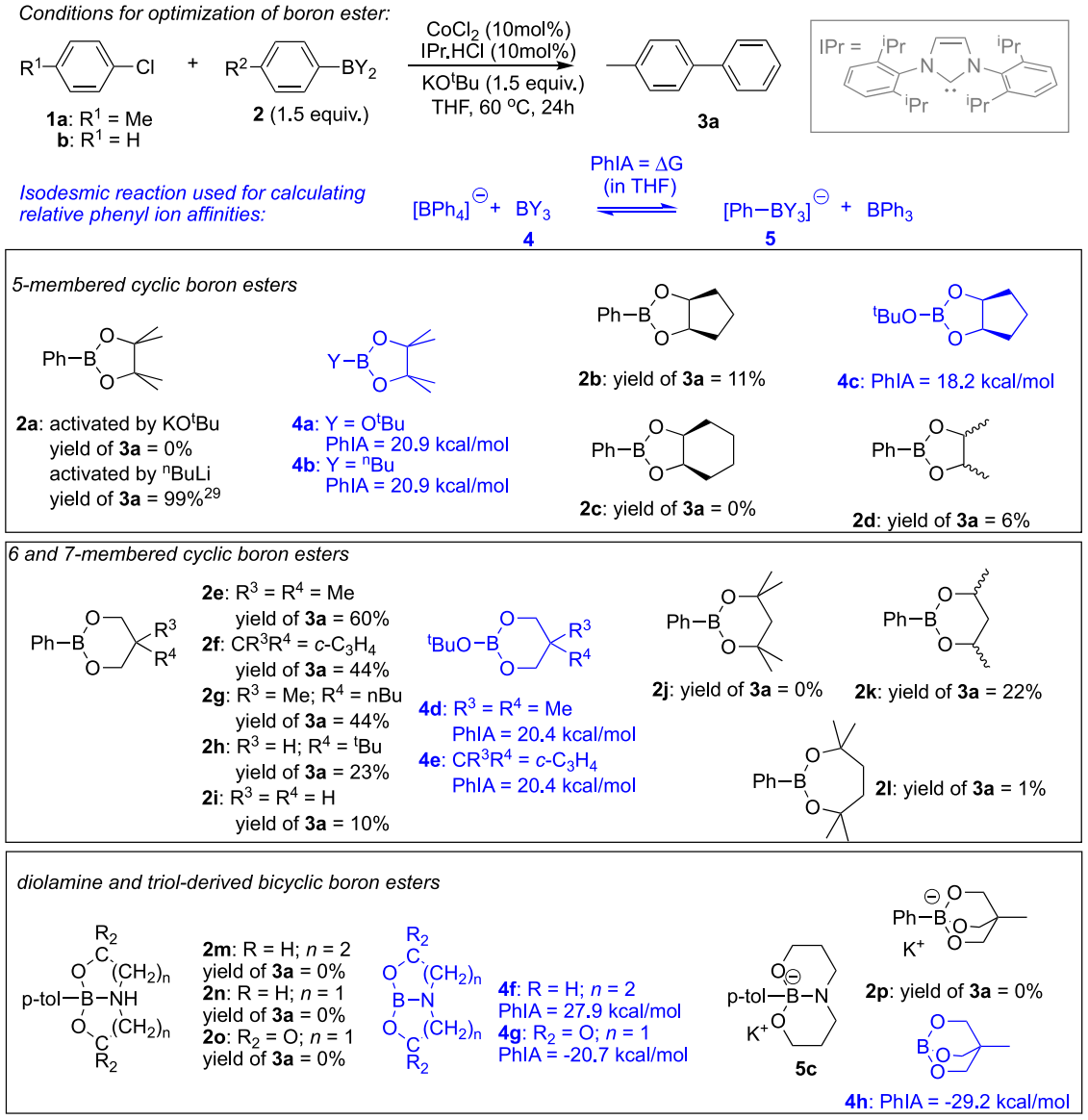

Figure 2. Effect of varying boronate on catalytic reaction (yields determined by G. C., dodecane internal standard) and calculated relative phenyl ion affinities (PhIA, B3LYP-D3/6-311+G**, implicit solvation by THF modeled using the CPCM; see the Supporting Information for full details).

and greater availability. Nickel[6−11] and copper-catalyzed[12−15] Suzuki biaryl cross-couplings are by far the most advanced. The iron-catalyzed cross-coupling of a range of sp^3-based electrophiles with aryl boron reagents has been reported,[16−22] but simple Suzuki biaryl coupling remains elusive,[23−25] with genuine examples limited so far to substrate-directed reactions.[26,27] While rare, cobalt-catalyzed Suzuki biaryl cross-coupling reactions are known.[24,28−31] Thus, aryl triflates or activated heteroaryl halides can be reasonably readily coupled with aryl boron esters activated with either organolithium reagents or, far more desirably, alkoxide salts.[28,30,31] Conversely, highly expedient, yet electronically challenging, aryl chloride substrates have only been shown to successfully couple when activated by harsher alkyl lithium bases.[29]

Resolving this dilemma would give the sought-after cobalt-catalyzed cross-coupling of aryl chlorides with aryl boron esters using practical bases. Accordingly, we re-examined the roles of alkoxide salts in this reaction and found that there is a fine balance between their ability to activate the aryl boron reagent and their intrinsic ability to inhibit or even poison the cobalt catalyst. We also uncovered a strong dependence of the catalytic activity on both the nature of the diol backbone of aryl boron ester and on the counterion of the alkoxide salt. With these critical pieces of information at hand, we were able to deliver the desired yet elusive biaryl cross-coupling reaction.

RESULTS AND DISCUSSION

Optimization Studies. The *N*-heterocyclic carbene ligand IPr (introduced as its HCl salt) was used throughout the initial optimization studies, as we had previously shown it to be useful in the related coupling reaction of aryl boronic ester activated by alkyl lithium reagents.[29] In the first instance, we examined the effect of varying the diolate backbone of the aryl boronic ester on the coupling reactions outlined in Figure 2; in particular, we were keen to see whether there is any relationship between the intrinsic thermodynamic propensity to transfer the aryl group from the boron center and performance in the catalytic reaction. This was done by examining the calculated relative phenyl ion affinities (PhIA)[32] of selected examples (density functional theory, B3LYP-D3/6-

https://dx.doi.org/10.1021/acscatal.0c05557
ACS Catal. 2021, 11, 3856−3866

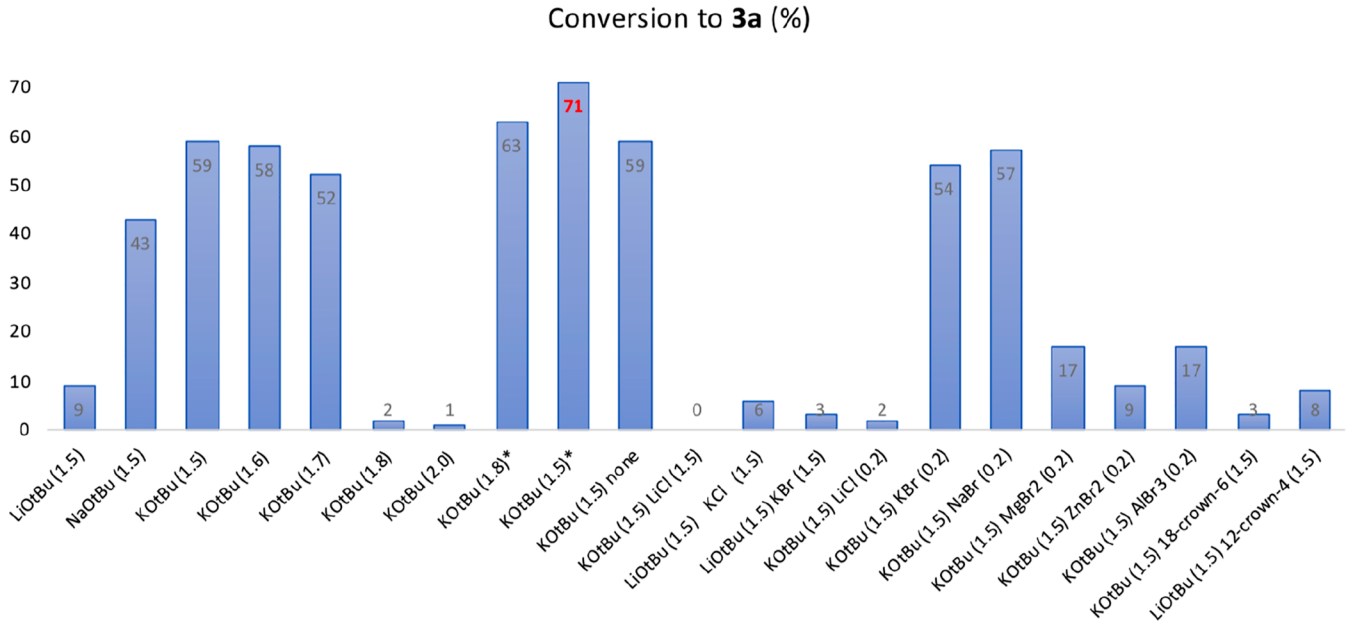

Figure 3. Selected data for the effect of variation of type and loading (equivalents with respect to **1a** loading, 1.5 equiv of boron ester **2e** used throughout) of alkali metal alkoxide and salt additives on the coupling of **1a** with **2e** to give **3a** (see Tables S4 and S5 for further data). The reaction with entries marked (*) employed 2.0 equiv of **2a** and 5 mol % of both $CoCl_2$ and IPr·HCl.

311+G**, implicit solvation by tetrahydrofuran (THF) modeled using the CPCM method; see Section 10 of the Supporting Information for full details) since this approach has previously been shown by Ingleson and co-workers to be a good proxy for transmetalation from boron to iron.[32] The PhIAs were determined according to the isodesmic processes outlined in Figure 2.

The initial reaction explored, the coupling of 4-chlorotoluene (**1a**) with the pinacol boronic ester **2a** activated with KO^{t}Bu acting as the base, unfortunately yielded none of the desired product **3a**. This is in sharp contrast with the analogous reaction using ^{n}BuLi as a base, which gave quantitative conversion to **3a**,[29] despite the identical thermodynamic propensity of the corresponding "ate" species [PhB(O^{t}Bu)(pin)]$^-$ to transfer a phenyl group, as judged by the calculated values for the relative PhIA. Small amounts of the desired product **3a** could be obtained by varying the α-substituents of the five-membered diolate motif (**2b** and **2d**). A more profound improvement was obtained on changing from five- to six-membered cyclic boron esters, with the boronic ester derived from neopentane diol (**2e**) giving a creditable 60% yield of **3a**. Notably, the calculated relative PhIA of **4d** is essentially identical to that of **4a**, indicating that the absence of activity observed with **2a** activated by KO^{t}Bu is not due to any intrinsic thermodynamic difference of the two substrates in their ability to transfer their phenyl groups to the cobalt center. Importantly, both **2e** and **2a** react in the same way with KO^{t}Bu to give the corresponding salts K[**5a**] (see below) and K[**5b**] (see the Supporting Information), indicating that differences in activation cannot account for the stark variation in performance in the catalytic reaction. Again, α-substitution of the diolate backbones of the six-membered boron esters proved deleterious, with no activity observed with tetra-methyl-substituted substrate **2j**, and almost no activity with the seven-membered analogue **2l**.

Ingleson and co-workers found the potassium salt **5c**, formed in situ by *N*-deprotonation of the dipropanolamine-derived boron ester **2m**, to be an excellent reagent for transfer of the 4-tolyl group to iron.[32] Despite the significantly increased thermodynamic propensity of **2m** to transfer an aryl group compared with **2e** (compare PhIAs of **4f** with **4d**), no activity was observed when this nucleophile was employed. Taking all of the calculated relative PhIA data together with the corresponding catalytic data, it is clear that there is no trend between the activity and the thermodynamic propensity of the activated aryl boron ester to transfer an aryl group. Instead, the profound variation in the activity must lie in more detailed kinetic considerations (see the Mechanistic Investigations section) and points strongly toward transmetalation being the key step to control in developing the catalytic transformation, as suggested previously by Chirik.[28]

As well as choosing cyclic aryl boronic ester, the correct choice of ligand, solvent, and alkoxide salt proved to be vital to the success of the reaction, as did the loading of the alkoxide salt. Table S2 summarizes the results obtained with various *N*-heterocyclic carbene, phosphine, imine, and amine-derived ligands. Of those tested, IPr and SIPr proved the stand-out ligands. Interestingly, all of the phosphines examined gave noticeably poorer performance than the use of $CoCl_2$ alone—which gave 11% of **3a** within 24 h, accompanied by significant amounts of homocoupled byproduct derived from the aryl boron ester (8%)—suggesting that these ligands actually inhibit cross-coupling. The fact that some activity, albeit low and unselective, was observed without added ligands prompted us to question whether cobalt nanoparticles were formed under these conditions; however, transmission electron microscopy (TEM) analysis indicated this was not the case (see the Supporting Information for details).

The use of 2-MeTHF or 1,4-dioxane in place of THF as solvent led to only a modest diminution in catalytic performance, while the use of either acetonitrile or dimethylformamide (DMF) led to a complete suppression of activity (Table S1).

https://dx.doi.org/10.1021/acscatal.0c05557
ACS Catal. 2021, 11, 3856−3866

Figure 3 summarizes selected data from a study on the influence of various alkoxide bases and salt additives on the coupling of **1a** with **2e** to give **3a** (see Tables S4 and S5 for full details). Of the alkoxides tested, *tert*-butoxide proved most effective, but the reaction was surprisingly sensitive to both the alkali metal counterion and the loading of the base. Thus, KO^{t}Bu worked well while the sodium analogue was less effective, and the lithium salt gave very poor activity. Critically, contrary to common practice in Suzuki cross-coupling, the alkoxide salt must absolutely not be used in significant excess as this proved highly deleterious to performance. Indeed, while increasing the loading of KO^{t}Bu from 1.5 to 1.7 equiv with respect to the aryl chloride **1a**, in reactions with 1.5 equiv of the boron ester **2e**, led to only a modest diminution in performance, increasing to 1.8 equiv led to an almost complete shutdown of the reaction.

An audit of the KO^{t}Bu in the latter reaction shows that 1.5 equiv of the base are used in a quantitative reaction with the boron ester **2e** to give the potassium boronate K[**5a**] (see the Supporting Information for details), the single-crystal X-ray structure of which is shown in Figure 4, while a further 0.1

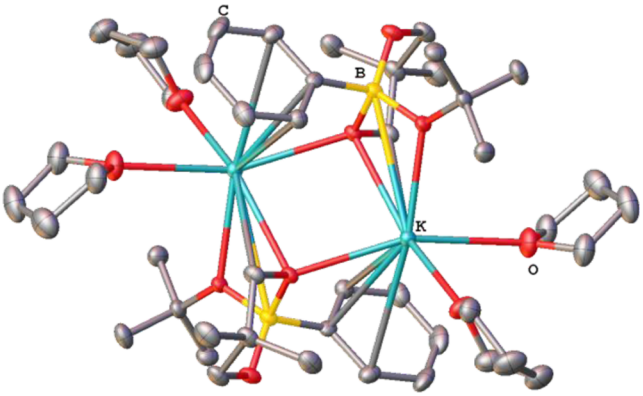

Figure 4. Single-crystal X-ray structure of the dimeric boronate K[**5a**] showing K$^+$−π-arene interactions. Thermal ellipsoids are set at 50% probability and hydrogen atoms are omitted for clarity.

equiv of the base are required to deprotonate the NHC precursor IPr·HCl. This leaves 0.2 equiv of KO^{t}Bu, or a ratio of cobalt to free KO^{t}Bu of 1:2, sufficient to almost completely suppress catalytic activity. Increasing the amount of the aryl boron ester **2e** to 2 equiv (using 1.8 equiv of the base) led to a complete recovery in activity even at a lower catalyst loading (5 mol %); meanwhile, reducing the KO^{t}Bu loading to 1.5 equiv while using 2 equiv of the boron ester led to the optimal conditions and a yield of **3a** of 71%. The mechanistic implications will be discussed in detail later, but it is clear from the optimization studies that both the nature of the counterion and the relative loading of the alkoxide salt have a profound influence on the success or otherwise of the catalytic reaction.

Substrate Scope. With optimized conditions in hand, we next turned our attention to the scope and limitations of the cross-coupling reaction, and the results from this study are summarized in Figure 5, while unsuccessful coupling reactions are presented in the Supporting Information, Section S4.2. Reasonable to good yields of the desired biaryl were obtained with alkyl-substituted aryl chlorides or naphthyl chloride substrates, although in the case of 1-phenyl naphthyl product **3f**, the naphthyl group was far better introduced via the aryl boronic ester coupling partner. 1-Chloro-4-fluorobenzene coupled well, although again the better performance was observed if **3h** was produced by swapping the substitution patterns between the aryl chloride and the boron ester. By contrast, both *para*-CF_3 and *ortho*-F groups on the aryl chloride gave disappointing yields of **3i** and **3j**, respectively. Similarly, aryl chlorides with ketone substituents gave modest to no yield. While the yield of **3n** was only modest, this was significantly better than the previously reported analogous coupling with aryl boron esters activated with ^{n}BuLi, where the cyano function is not tolerated, but not as good as reported by Duong and co-workers for this class of substrate.[29,30] In sharp contrast with the general trend observed in palladium-catalyzed Suzuki cross-coupling, electron-rich aryl chlorides with alkoxy or dialkylamino groups gave reasonable to good yields of the desired biaryls.

Heteroaryl chlorides based on pyridine or benzothiazole were tolerated, although the latter proved to be the exception to the more general observation that sulfur-based moieties are not tolerated on either coupling partner. Indeed, control reactions between **1a** and **2e** were poisoned by the addition of 1 equiv of either thiophene or methyl phenyl thioether. Broadly speaking, variation in the para-substituent on the aryl boron ester indicated somewhat surprisingly that electron-withdrawing groups tended to give better performance than electron-donating groups, an observation borne out by a Hammett analysis (see the Mechanistic Investigations section). Meanwhile, the introduction of a methoxy into the ortho-position of the aryl nucleophile gave enhanced performance suggesting that in this instance neighboring group participation may play a positive role. Indeed, the effect proved sufficiently large to overcome the poor performance associated with a *para*-CF_3 on the aryl chloride substrate (compare **3aa** with **3i** and **3ac**).

Mechanistic Investigations. *Influence of the Base.* As outlined in Figure 3, both the counterion and loading of the *tert*-butoxide base have a profound effect on activity. To probe the role of the counterion further, we examined the effect of additives on the catalytic reaction, and selected results are shown in Figure 3 (for full results, see Table S5). It can clearly be seen that not only does the use of LiO^{t}Bu in place of KO^{t}Bu inhibit the reaction, the same inhibition is seen on addition of stoichiometric or catalytic amounts of LiCl to reactions with KO^{t}Bu acting as the base. Furthermore, the addition of stochiometric KBr to the reaction with LiO^{t}Bu as a base does not restore activity. Evidently lithium salts inhibit the catalysis however introduced. Inhibition is also seen when catalytic amounts of $MgBr_2$, $ZnBr_2$, or $AlBr_3$ are added to reactions using KO^{t}Bu as the base, while the addition of KBr or NaBr has no real impact, ruling out the possibility of a deleterious role played by bromide.

It is apparent from ^{1}H NMR spectroscopic investigations that there is a significant difference between how Li$^+$ and K$^+$ interact with the anion **5a**$^-$ (see the Supporting Information for details); meanwhile, the X-ray structure for K[**5a**] (Figure 4) contains K$^+$−π interactions, which are absent in analogous structures with lithium or sodium counterions.[33−35] It is tempting to conclude that the observed activity order for MO^{t}Bu of K > Na > Li may be due to increasing oxophilicity of the counterions of the boronate salt: it may be more challenging to replace the alkali metal with the cobalt catalyst in a transmetalation step (see below). However, the fact that even a catalytic amount of Li$^+$ suppresses activity suggests that

https://dx.doi.org/10.1021/acscatal.0c05557
ACS Catal. 2021, 11, 3856−3866

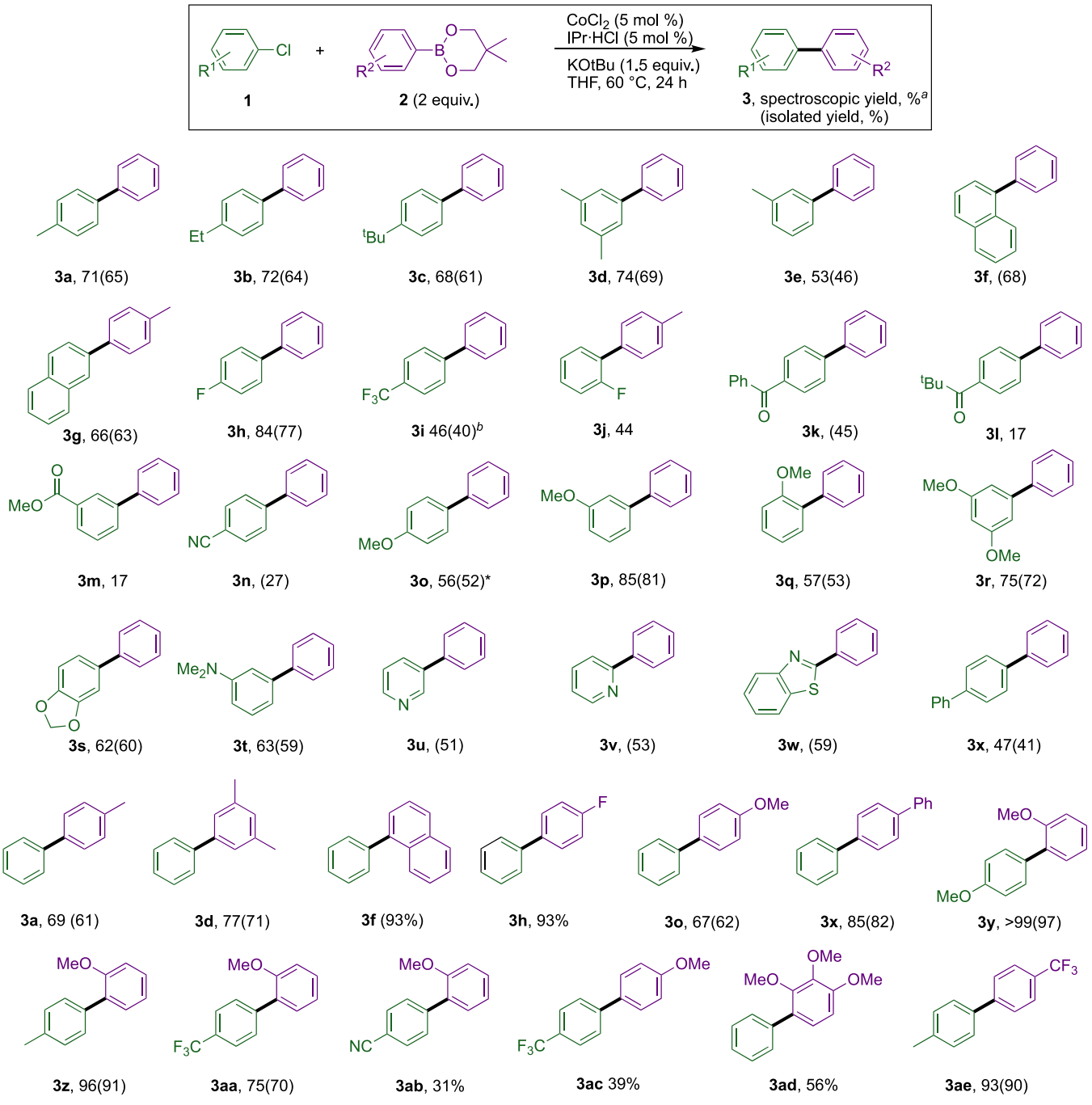

Figure 5. Selected Suzuki cross-coupling reaction. Conditions: $CoCl_2$ (0.025 mmol), IPr·HCl (0.025 mmol), aryl chloride (0.5 mmol), KO^{t}Bu (0.75 mmol), aryl boron ester (1.0 mmol), THF (3 mL), 60 °C, and 24 h.[a] Determined by ^{1}H NMR (1,4-C_6H_4-NO_2 internal standard) or GC (dodecane internal standard). * 10 mol % of precatalyst used. Unsuccessful reactions are given in the Supporting Information, Section S4.2.

the issue is more likely due to the lithium ion interacting deleteriously with the cobalt center in addition to or instead of simply with the boronate. One way this might occur is via interaction of the counterion with alkoxide ligands on the cobalt center. To probe this further, we investigated the nature of the species formed on reacting representative cobalt species with MO^{t}Bu salts.

The reaction of (IPr)$CoCl_2$ (formed in situ) with 3 equiv of KO^{t}Bu yielded the potassium salt of the NHC-free ate complex $[Co(O^tBu)_3]^-$ (**6**$^-$, Figure 6). A genuine sample of K[**6**] was prepared according to modification of a literature method for comparison purposes,[36] by the reaction of $CoCl_2$ with 3 equiv of the base. It is clear that the NHC ligand is readily displaced by a *tert*-butoxide ligand. No reaction was observed between the complex K[**6**] with an excess of the NHC ligand. Displacement of the NHC ligand also occurred when only 2 equiv of KO^{t}Bu were employed, giving a highly insoluble purple product, **7**, that could also be prepared by either the reaction of $CoCl_2$ with 2 equiv of KO^{t}Bu or $[Co(N(SiMe_3)_2)]$ with 2 equiv of *tert*-butanol.

The powder X-ray diffraction (XRD) pattern of **7** (Figure 7) shows reflections at 2θ = 18.0, 31.6, 36.5, 37.0, and 41.3°. Based on the reaction stoichiometries and the highly insoluble nature of the product, we suggest that **7** is a polymer of

https://dx.doi.org/10.1021/acscatal.0c05557
ACS Catal. 2021, 11, 3856−3866

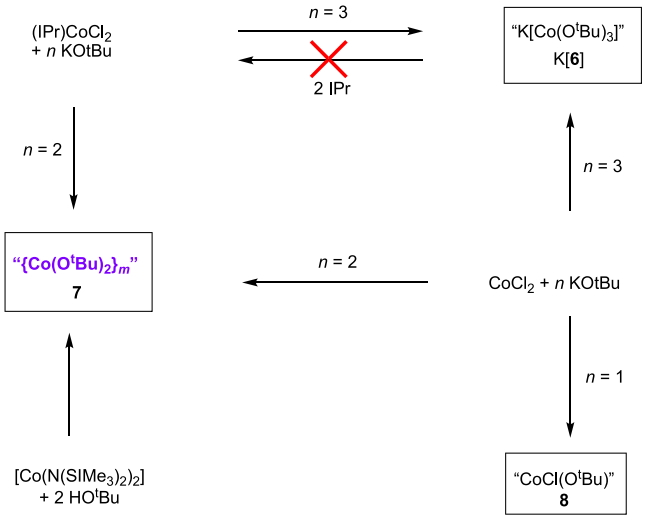

Figure 6. Reactions of cobalt precursors with KO^{t}Bu (THF, r.t. 30 min).

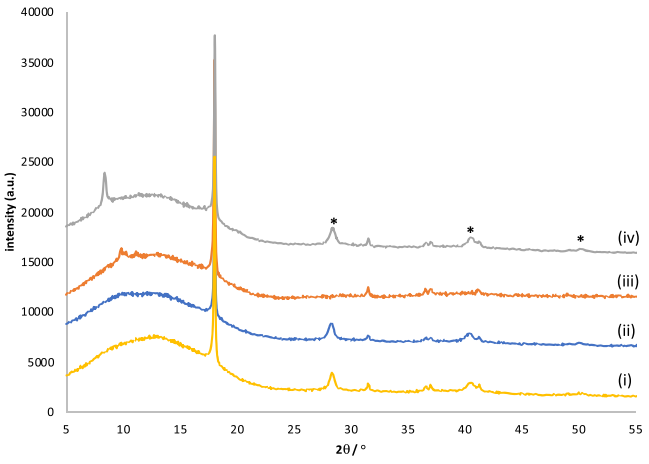

Figure 7. Powder XRD data for samples of **7** obtained by: (i) reaction of $CoCl_2$ with 2 KO^{t}Bu; (ii) reaction of (IPr)$CoCl_2$ with 2 KO^{t}Bu; (iii) reaction of $[Co(N(SiMe_3)_2)_2]$ with 2 HO^{t}Bu; and (iv) at the end of a representative catalytic reaction, * indicates reflections due to coprecipitated KCl.

$[Co(O^tBu)_2]$ in which four-coordinate cobalt centers are bridged by two *tert*-butoxide ligands. The same highly insoluble purple precipitate is observed toward the end of many of the catalytic transformations.

Interestingly, unlike "ligand free" $CoCl_2$, which showed some catalytic activity—albeit low yielding and unselective (see above)—K[**6**] proved not to be a viable precatalyst under NHC-free conditions when 1.5 equiv of aryl boron ester **2e** and 1.5 equiv base (with respect to aryl chloride) were used. However, when the amount of the boron ester was increased to 2 equiv, in the reaction catalyzed by K[**6**], then 24% of the cross-coupled product was obtained along with 24% of biphenyl. This provides clear evidence that the boron ester can "mop up" the alkoxide even when it is coordinated to cobalt. The inactivity of K[**6**] in the absence of excess **2e**, coupled with the observation that the complex does not react with free IPr, and slowly degrades to **7** when heated with IPr·HCl, suggests that both the ligand and one or both of the coupling partners are required to transform **6** into a catalytically viable intermediate. This is supported by the observation that complex K[**6**] is an active precatalyst in the presence IPr·HCl, giving 51% of **3a**. Taken together, it is clear that for good activity the NHC ligand is required, and that a stoichiometric or excess of aryl boron ester is needed with respect to total alkoxide loading to prevent catalyst deactivation.

The previously reported single-crystal X-ray structure of K[**6**] shows that the molecule is dimeric with two-terminal and two-bridging alkoxide ligands per cobalt, with each potassium coordinated by one of the bridging alkoxides and two of the terminal alkoxides, one from each Co (structure type **I**, Figure 8).[36] The structural type **I** was also reported for Na[**6**];[36]

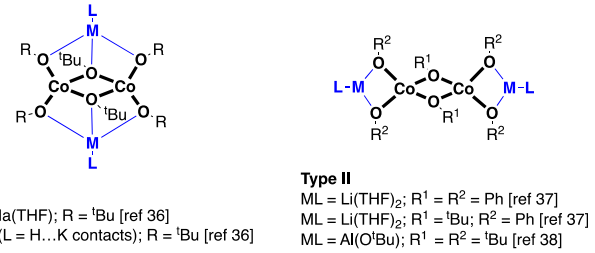

Type I
ML = Na(THF); R = ^{t}Bu [ref 36]
M = K (L = H…K contacts); R = ^{t}Bu [ref 36]

Type II
ML = Li(THF)$_2$; $R^1 = R^2$ = Ph [ref 37]
ML = Li(THF)$_2$; R^1 = ^{t}Bu; R^2 = Ph [ref 37]
ML = Al(O^{t}Bu); $R^1 = R^2$ = ^{t}Bu [ref 38]

Figure 8. Structural variation in trisalkoxide cobaltate anions with differing metal counterions.

meanwhile, smaller, more oxophilic metals have been shown to give structure type **II** in related complexes in which the metal is coordinated by the two terminal alkoxides.[37,38]

^{1}H NMR spectroscopy of a THF solution of K[**6**] shows only two paramagnetically shifted butoxide peaks, 21.5 and −37.3 ppm in a 2:1 ratio, consistent with the dimeric structure being preserved in solution; meanwhile, the spectra of Na[**6**] and Li[**6**] show multiple peaks for the *tert*-butoxide ligands, suggesting that in the solution a variety of oligomeric species are obtained (see Figures S37 and S38). When LiCl, $MgBr_2$, or $ZnBr_2$ were added to the solutions of K[**6**], then once again multiple alkoxide environments were observed; conversely, the addition of NaBr had no effect on the spectrum. Taken together, the NMR data suggest that while the potassium salt cleanly gives a single species in the solution, harder, more oxophilic cations give complex mixtures and can displace the potassium salt. The exception is sodium which, despite giving complex mixtures on its own, is unable to displace potassium, suggesting weaker interaction with the alkoxides of the more heavily aggregated species.

The relatively weak binding of K^+ and Na^+ to the cobalt alkoxide species may well account for the observed activity with these counterions, while the relatively strong binding of more oxophillic cations my explain their inhibitory effect. We cannot preclude the possibility that one or more of the multiple alkoxide peaks observed in the ^{1}H NMR spectra derived from heteroleptic "CoX(O^{t}Bu)" species (X = Cl, Br); indeed, such species have been crystallographically characterized previously.[39−41] The ^{1}H NMR spectrum of a reaction between $CoCl_2$ with only 1 equiv of KO^{t}Bu shows a single peak at 41.5 ppm, suggestive of the formation of a mono-alkoxide complex, **8** (Figure 6); however, it is not possible to comment on whether this species is a neutral complex or an ate species, nor whether it is monomeric or oligomeric, beyond noting that the shift is in the same general region of that observed for the terminal *tert*-butoxide ligands in K[**6**].

So far, the data do not suggest a positive role for potassium, rather a deleterious role for more oxophilic cations; however,

https://dx.doi.org/10.1021/acscatal.0c05557
ACS Catal. 2021, 11, 3856−3866

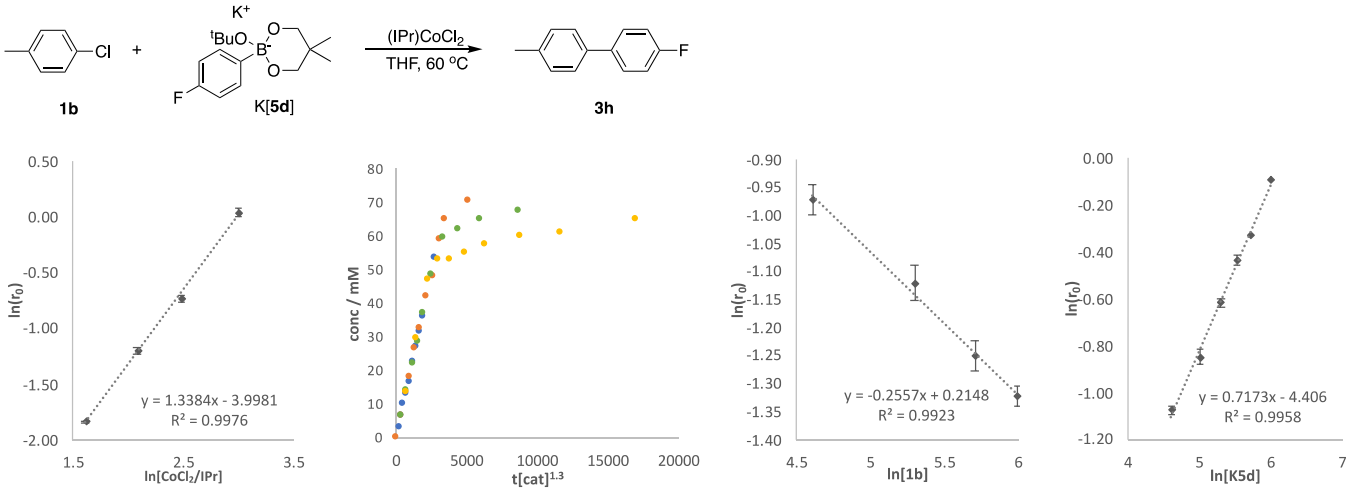

Figure 9. Kinetic investigations. Full details are given in the Supporting Information.

the explanation cannot be this straightforward. If the only role for the cation were that it hampers reactivity, then sequestering the cation in an appropriate crown ether would be expected to have little or no influence on activity in the case of K^+ yet significant benefit in reactions inhibited by Li^+. However, this is not the case, addition of 1 equiv of 18-crown-6 per potassium in a reaction with KO^{t}Bu switches off activity (Figure 3), while the addition of 12-crown-4 in a reaction with LiO^{t}Bu has no effect on performance.

Summarizing, when KO^{t}Bu is used as the base, an excess of two or more free alkoxides per cobalt must be avoided to prevent the formation of either the inactive ate complex K[**6**], which needs to be subsequently transformed into an active species in the presence of free NHC ligand and one or more of the components of the catalytic reaction, or worse the formation of the highly insoluble polymer **7**, which represents a catalyst termination process. Replacing potassium with harder more oxophilic cations is highly deleterious to performance.

Catalyst Activation. As can be seen in Figures S1 and S2, the catalytic reaction is subject to an induction period of around 190 min, during which a significant proportion of the side-product, biphenyl (**9**), is produced by a homocoupling of the nucleophilic substrate. The formation of **9** is indicative of a reductive elimination from cobalt, and, in the absence of the electrophile, the amount produced can be used as a proxy to determine the lowest bulk oxidation state that can be thermodynamically accessed on the metal under the reaction conditions.[42] Meanwhile, the time frame in which it is produced in the absence of the electrophile can help determine the kinetically most relevant bulk oxidation state. Here, approximately 0.7 electrons per cobalt are released during the reductive activation of the NHC-containing precatalyst, corresponding to an approximately 70% conversion to an average bulk oxidation state of Co(I) for the activated catalyst. Examining catalytic reaction mixtures formed in the presence or absence of the NHC ligand by TEM did not reveal the presence of any cobalt nanoparticles (see the Supporting Information, Section S11). We previously found that homogeneous cobalt(0) SIPr complexes could be trapped using alkenes and dienes when reducing the precatalyst mixture with BuLi-activate boronates;[29] however, this is not the case here (see the Supporting Information, Section S8.1), indicating first that the aryl boronate K[**5a**] is less reducing than the boronate formed on reaction of **2a** with butyllithium and second that any catalytic manifold that requires access to the Co(0) oxidation state can be excluded here.

Kinetic and Computational Investigations. Figure 9 summarizes the kinetic data obtained for the coupling of chlorobenzene **1b** with the preformed borate salt K[**5d**] using the precatalyst IPrCoCl$_2$, formed in situ by stirring CoCl$_2$ with IPr for 15 min before the start of catalysis. Interestingly, using the mixture of preformed carbene complex and preformed borate significantly reduced the induction period to around 20 min, with essentially no turnover observed before this point. While the use of the initial rate method in catalytic reactions with induction periods can be problematic, the essentially complete lack of formation of **3h** during the induction period followed by clear regions of linear increase in the concentration of **3h** vs time (typically to between 10 and 25% conversion to product, see Figures S5−S7) gave us reasonable confidence in the use of this approach, when applied to the linear regions of product growth.

The initial rate analysis shows that the rate of catalysis has a slightly greater than first-order dependence (1.3) on the concentration of the precatalyst, an observation confirmed by variable time normalization analysis (VTNA),[43] which both showed that the same order holds true throughout a significant proportion of the reaction and helped vindicate our application of the initial rates method to the postinduction phase region of catalysis. Meanwhile, a positive order dependence of approximately 0.7 was observed for borate. Surprisingly, the order in aryl chloride proved to be slightly negative (approx. −0.3). Clearly, the oxidative addition of **1a** is not the rate-limiting step, while the slight negative order suggests a secondary, inhibitory role for the substrate, possibly by the formation of an off-cycle cobalt adduct, which might also explain greater than first-order dependence on the concentration of precatalyst. The positive order dependence on the borate K[**5d**] indicates its prominent role either in the rate-determining process or in an unfavorable equilibrium prior to this step.

Linear free-energy analyses were performed varying the para-substituents on both the aryl chloride and the aryl boronic ester (Figure 10). On varying the electronics of the ester **2a**, a strongly positive value for ρ was obtained, indicating either the build-up of negative charge or a loss of positive charge in the rate-determining step.

https://dx.doi.org/10.1021/acscatal.0c05557
ACS Catal. 2021, 11, 3856−3866

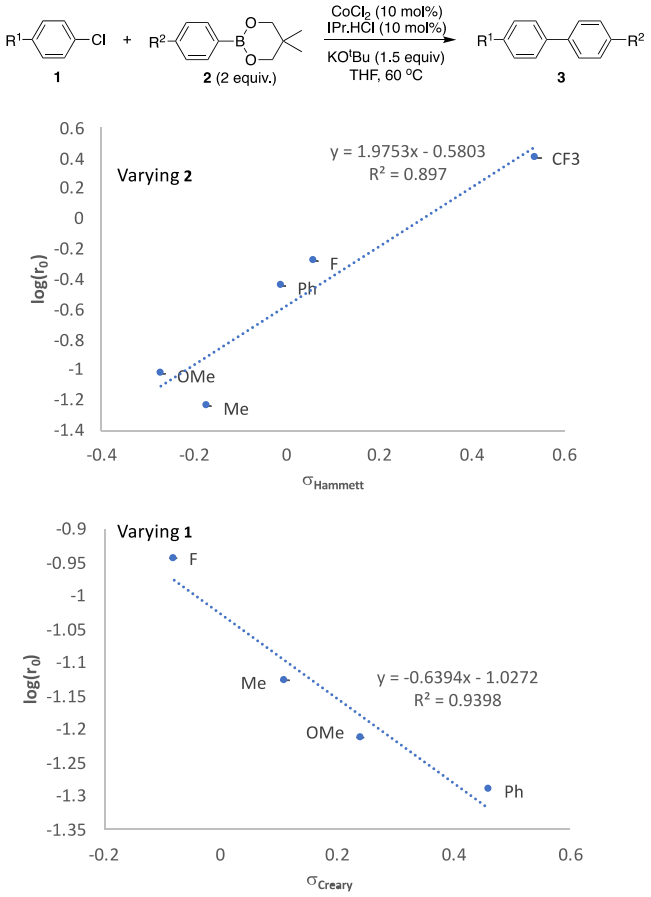

Figure 10. Linear free-energy studies.

This is distinct from transmetalation from aryl boronic acids to palladium, which typically show a negative ρ.[44,45] While oxidative addition is not the rate-determining step, the observed dependence of rate on the nature of the p-substituent of the aryl chloride indicates that the rate-determining process occurs after the oxidative addition step and that the aryl group is a component part of the intermediate prior to the slow step.

Unlike with the aryl on the boronate, the rate does not show a simple Hammett dependence on the p-substituent of aryl chloride, but rather a dependence on the Creary scale,[46] suggesting radical character. A radical-based reductive elimination would show a radical stability dependence for both aryl groups, which is clearly not the case, and can thus be discounted, as can any other form of reductive elimination being the slow step, as the profoundly different electronic influences of the two aryls are essentially irreconcilable in such a scenario: reductive elimination of aryl−aryl′ from any intermediate Co(aryl)(aryl′) cannot give one trend for substitution of aryl and a separate trend for the substation of aryl′. Indeed, the data indicate that while both aryl groups are present in an intermediate immediately prior to the rate-determining transformation, or in equilibrium with such a species, they are in profoundly different environments.

To probe the mechanism further, we undertook a computational investigation into the catalytic manifold. All calculations were performed using Orca 4.2,[47,48] employing the B3LYP functional.[49−52] with Grimme's D3 dispersion correction with Becke−Johnson damping[53] and were accelerated by the use of the RIJCOSX approximation.[54] Intermediates and transition states were optimized using the def2-SVP basis sets, single-point energies were separately determined using the larger def2-TZVP basis set, while THF solvation was accounted for by a single-point calculation using the conductor-like polarizable continuum model.[55] For full details, see the Supporting Information, Section S10.

Figure 11 summarizes the key results from the computational study. For simplicity, we investigated the manifold using the free boronate ion $\mathbf{6}^-$, rather than its potassium salt. While the mechanistic studies above indicate that the role and nature of the alkali metal ion are critical to success, too many variables and unknowns including speciation and highly variable levels of solvation render realistic modeling of the role(s) of the counterion beyond the scope of the current study. We instead focussed more broadly on determining a representative catalytic manifold, focussing in particular on the likely spin states of the intermediates as well as the likely slow transformation.

The intermediate LCoCl, $\mathbf{I_A}$, was used as a model for the Co(I) species formed *in situ*. While we cannot rule out mono-alkoxide-containing analogues or ate species, for simplicity, we decided this would act as a useful and representative starting point. Modeling the THF-containing analogues of $^{HS}\mathbf{I_A}$ (see Figure S44) showed that mono-adduct $^{HS}\mathbf{I_A}$(THF) was just under 3 kcal/mol higher in energy, while neither $^{HS}\mathbf{I_A}$(THF)$_2$ nor $^{HS}\mathbf{I_A}$(THF)$_3$ converged, with both failed optimizations indicating dissociation of one or two THF ligands, respectively. As can be seen in Figure 11, high spin (S = 1) $^{HS}\mathbf{I_A}$ undergoes coordination of chlorobenzene, **1b**, to give intermediate $^{HS}\mathbf{I_B}$, followed by oxidative addition via the transition state $^{HS}\mathbf{TS_{OA}}$ to give the intermediate spin (S = 1) Co(III) species $^{IS}\mathbf{I_C}$. Overall, this sequence is exergonic by around 3 kcal/mol compared with the starting materials. Explicit solvation of $^{HS}\mathbf{I_B}$ with 1 equiv of THF gave an intermediate $^{HS}\mathbf{I_B}$(THF) that was marginally (1.2 kcal/mol) lower in energy; however, the analogous subsequent transition state $^{HS}\mathbf{TS_{OA}}$(THF) could not be located. Figure S44 outlines the analogous oxidation addition pathway starting with the low-spin Co(I), $^{LS}\mathbf{I_A}$. Here, explicit THF coordination proved beneficial; however, the pathway remained far too high in energy compared with the HS route to be operative; furthermore, we were unable to locate an appropriate transition state for oxidative addition on this surface.

Subsequent steps involving Co(III) were modeled on all three possible spin surfaces: S = 0 (low spin, LS); S = 1 (intermediate spin, IS), and S = 2 (high spin, HS). In all cases, the intermediates and transitions states on the IS pathway were significantly lower in energy than either the HS or LS analogues. Meanwhile for Co(I) intermediates and transition states, HS (S = 1) is preferred over LS (S = 0), indicating that the catalytic cycle essentially lies entirely on the triplet manifold.

The coordination of the "naked" borate anion $\mathbf{6}^-$ and displacement of the chloride ligand in intermediate $^{IS}\mathbf{I_C}$ to give $^{IS}\mathbf{I_D}$ is unfavorable, while the subsequent transition state for transmetalation ($^{IS}\mathbf{TS_{TM}}$) represents the turn-over frequency-determining transition state (TDTS).[56] Subsequent reductive elimination and product loss processes complete the cycle and proceed smoothly on the triplet surface, with the reformation of $^{HS}\mathbf{I_A}$ and liberation of product representing the turn-over frequency-determining intermediate (TDI), which gives a calculated energetic span of 27.9 kcal/mol for the catalytic cycle.[56]

https://dx.doi.org/10.1021/acscatal.0c05557
ACS Catal. 2021, 11, 3856−3866

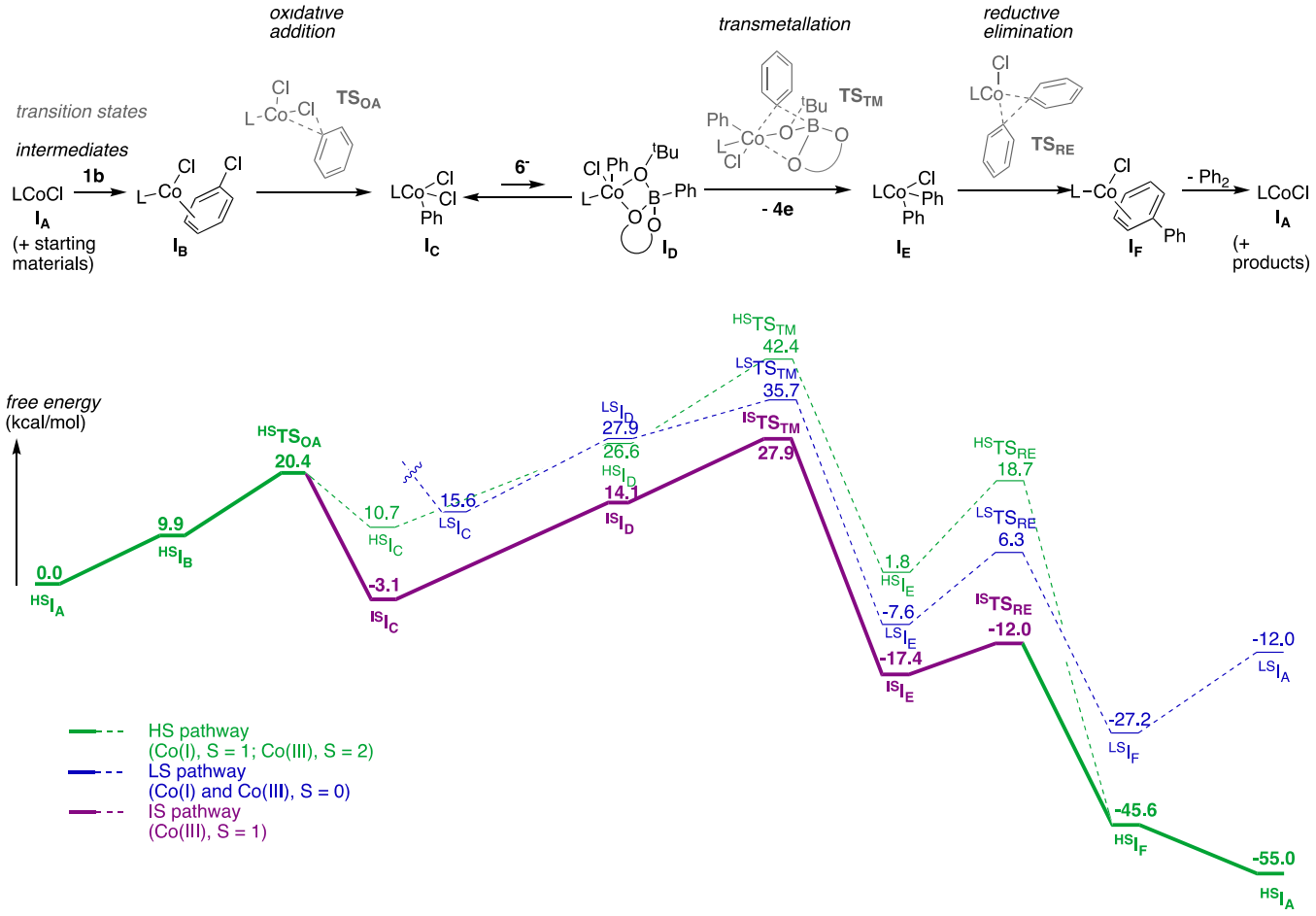

Figure 11. Selected data from the density functional theory investigation of the proposed catalytic cycle. Further data, including alternative pathways starting with a low-spin state for $\mathbf{I_A}$ and the effect of explicit solvation, are presented in the Supporting Information.

The determination of $^{IS}\mathbf{TS_{TM}}$ as the TDTS marries well with the catalytic and mechanistic observations outlined above. Examining the structure of the TDTS, $^{IS}\mathbf{TS_{TM}}$, it is clear that reducing the size of the boron diolate ring would increase ring strain in the $Co(O)_2B$ moiety, disfavoring the transmetalation, consistent with the observed pronounced deleterious effect on changing from a six- to a five-membered B-diolate. Meanwhile, variation of both the aryl on the cobalt (derived from the aryl chloride substrate) and the aryl on the boron center in the transition state $^{IS}\mathbf{TS_{TM}}$ would be expected to impact upon the rate of catalysis, as observed in the kinetic and Hammett investigations above, with quite distinct electronic influences anticipated and obtained. The intermediate spin Co(III) center is a triplet diradical; therefore, it is perhaps not surprising that the relative rates associated with processes that lead to changes in cobalt's coordination sphere might well be expected to display a Creary dependence on the para-functional groups in the linear free-energy analysis. The observed positive value for ρ obtained on varying the para-substituents on the boron center indicate either the build-up of negative charge or a loss of positive charge in the TDTS. This may well reflect changes in the location of the potassium counterion *en route* to the TDTS; the modeling of which is beyond the scope of the current study.

CONCLUSIONS

In conclusion, we have instigated the cobalt-catalyzed Suzuki coupling of aryl chloride substrates with aryl boron esters activated by alkoxide bases. As has been previously suggested,[28] the challenging step in the manifold proved to be transmetalation, but we have shown that the problems associated with this exacting transformation can be overcome. Key to success is (i) the correct choice of diolate residue on the aryl boron ester, (ii) the nature of the counterion of the alkoxide base, with potassium *tert*-butoxide proving to be best under our conditions, and (iii) tight control of the stoichiometry of the base with respect to the aryl boron ester. As yet we have not been able to fully unpick the role(s) of the counterion on the reaction, although it seems highly likely from the data obtained that the counterion is required in the formation of a boronate−cobalt cluster, a key intermediate in the slow transmetalation step. Whether transmetalation occurs from this point or whether solvated potassium chloride is fully or partially extruded prior to aryl transfer has not yet been established, although the inhibitory role of lithium suggests that overly tight coordination of the counterion may inhibit such a process and thus the catalytic reaction. Now that the major obstacle to transmetalation has been cleared in the cobalt-catalyzed Suzuki biaryl cross-coupling reaction, future developments must focus on producing higher activity catalysts that can act as genuine challengers to the supremacy of palladium in the reaction.

https://dx.doi.org/10.1021/acscatal.0c05557
ACS Catal. 2021, 11, 3856−3866

■ ASSOCIATED CONTENT

Supporting Information

The Supporting Information is available free of charge at https://pubs.acs.org/doi/10.1021/acscatal.0c05557.

All experimental details, including syntheses, catalytic procedures, kinetic analyses, computational details, spectroscopic data, and crystallographic data (CIF) (PDF)

■ AUTHOR INFORMATION

Corresponding Author

Robin B. Bedford − *School of Chemistry, University of Bristol, Bristol BS8 1TS, U.K.;* orcid.org/0000-0002-8021-8768; Email: r.bedford@bristol.ac.uk

Authors

Sanita B. Tailor − *School of Chemistry, University of Bristol, Bristol BS8 1TS, U.K.*

Mattia Manzotti − *School of Chemistry, University of Bristol, Bristol BS8 1TS, U.K.;* orcid.org/0000-0001-9058-8087

Gavin J. Smith − *School of Chemistry, University of Bristol, Bristol BS8 1TS, U.K.*

Sean A. Davis − *School of Chemistry, University of Bristol, Bristol BS8 1TS, U.K.*

Complete contact information is available at: https://pubs.acs.org/10.1021/acscatal.0c05557

Author Contributions

†S.B.T. and M.M. contributed equally to this work.

Notes

The authors declare no competing financial interest.

■ ACKNOWLEDGMENTS

The authors thank the following for supporting the project: the EPSRC for provision of a studentship (to S.B.T.), the provision of a studentship through the EPSRC Centre for Doctoral Training in Catalysis (to M.M.), and the Erasmus+ Fund of the European Union for financial support (G.J.S.).

■ REFERENCES

(1) Miyaura, N.; Suzuki, A. Palladium-catalyzed cross-coupling reactions of organoboron compounds. *Chem. Rev.* **1995**, *95*, 2457−2483.

(2) Valente, C.; Organ, M. G. The Contemporary Suzuki-Miyaura Reaction. In *Boronic Acids*; Hall, D. G., Ed.; Wiley-VCH: Weinheim, Germany, 2011; pp 213−262.

(3) Torborg, C.; Beller, M. Recent applications of palladium-catalyzed coupling reactions in the pharmaceutical, agrochemical, and fine chemical industries. *Adv. Synth. Catal.* **2009**, *351*, 3027−3043.

(4) Garrett, C. E.; Prasad, K. The art of meeting palladium specifications in active pharmaceutical ingredients produced by Pd-catalyzed reactions. *Adv. Synth. Catal.* **2004**, *346*, 889−900.

(5) Albrecht, M.; Bedford, R.; Plietker, B. Catalytic and Organometallic Chemistry of Earth-Abundant Metals. *Organometallics* **2014**, *33*, 5619−5621.

(6) Han, F.-S. Transition-metal-catalyzed Suzuki−Miyaura cross-coupling reactions: a remarkable advance from palladium to nickel catalysts. *Chem. Soc. Rev.* **2013**, *42*, 5270−5298.

(7) Mastalir, M.; Stöger, B.; Pittenauer, E.; Allmaier, G.; Kirchner, K. Air-stable triazine-based Ni(ii) PNP pincer complexes as catalysts for the Suzuki−Miyaura cross-coupling. *Org. Lett.* **2016**, *18*, 3186−3189.

(8) Zhou, J.; Berthel, J. H. J.; Kuntze-Fechner, M. W.; Friedrich, A.; Marder, T. B.; Radius, U. NHC nickel-catalyzed Suzuki−Miyaura cross-coupling reactions of aryl boronate esters with perfluorobenzenes. *J. Org. Chem.* **2016**, *81*, 5789−5794.

(9) Shi, S.; Meng, G.; Szostak, M. Synthesis of biaryls through nickel-catalyzed Suzuki−Miyaura coupling of amides by carbon−nitrogen bond cleavage. *Angew. Chem., Int. Ed.* **2016**, *55*, 6959−6963.

(10) Malan, F. P.; Singleton, E.; van Rooyen, P. H.; Landman, M. Facile Suzuki-Miyaura coupling of activated aryl halides using new CpNiBr(NHC) complexes. *J. Organomet. Chem.* **2016**, *813*, 7−14.

(11) Shields, J. D.; Gray, E. E.; Doyle, A. G. A modular, air-stable nickel precatalyst. *Org. Lett.* **2015**, *17*, 2166−2169.

(12) Thapa, S.; Shrestha, B.; Gurung, S. K.; Giri, R. Copper-catalysed cross-coupling: an untapped potential. *Org. Biomol. Chem.* **2015**, *13*, 4816−4827.

(13) Gurung, S. K.; Thapa, S.; Shrestha, B.; Giri, R. Copper-catalysed cross-couplings of arylboronate esters with aryl and heteroaryl iodides and bromides. *Org. Chem. Front.* **2015**, *2*, 649−653.

(14) Zhou, Y.; You, W.; Smith, K. B.; Brown, M. K. Copper-catalyzed cross-coupling of boronic esters with aryl iodides and application to the carboboration of alkynes and allenes. *Angew. Chem., Int. Ed.* **2014**, *53*, 3475−3479.

(15) Gurung, S. K.; Thapa, S.; Kafle, A.; Dickie, D. A.; Giri, R. Copper-catalyzed Suzuki−Miyaura coupling of arylboronate esters: transmetalation with (PN)CuF and identification of intermediates. *Org. Lett.* **2014**, *16*, 1264−1267.

(16) Bedford, R. B.; Hall, M. A.; Hodges, G. R.; Huwe, M.; Wilkinson, M. C. Simple mixed Fe−Zn catalysts for the Suzuki couplings of tetraarylborates with benzyl halides and 2-halopyridines. *Chem. Commun.* **2009**, *42*, 6430−6432.

(17) Hatakeyama, T.; Hashimoto, T.; Kondo, Y.; Fujiwara, Y.; Seike, H.; Takaya, H.; Tamada, Y.; Ono, T.; Nakamura, M. Iron-Catalyzed Suzuki−Miyaura Coupling of Alkyl Halides. *J. Am. Chem. Soc.* **2010**, *132*, 10674−10676.

(18) Hashimoto, T.; Hatakeyama, T.; Nakamura, M. Stereospecific Cross-Coupling between Alkenylboronates and Alkyl Halides Catalyzed by Iron−Bisphosphine Complexes. *J. Org. Chem.* **2012**, *77*, 1168−1173.

(19) Hatakeyama, T.; Hashimoto, T.; Kathriarachchi, K. K. A. D. S.; Zenmyo, T.; Seike, H.; Nakamura, M. Iron-Catalyzed Alkyl−Alkyl Suzuki−Miyaura Coupling. *Angew. Chem., Int. Ed.* **2012**, *51*, 8834−8837.

(20) Bedford, R. B.; Brenner, P. B.; Carter, E.; Carvell, T. W.; Cogswell, P. M.; Gallagher, T.; Harvey, J. N.; Murphy, D. M.; Neeve, E. C.; Nunn, J.; Pye, D. R. Expedient Iron-Catalyzed Coupling of Alkyl, Benzyl and Allyl Halides with Arylboronic Esters. *Chem. - Eur. J.* **2014**, *20*, 7935−7938.

(21) Bedford, R. B.; Brenner, P. B.; Carter, E.; Clifton, J.; Cogswell, P. M.; Gower, N. J.; Haddow, M. F.; Harvey, J. N.; Kehl, J. A.; Murphy, D. M.; Neeve, E. C.; Neidig, M. L.; Nunn, J.; Snyder, B. E. R.; Taylor, J. Iron Phosphine Catalyzed Cross-Coupling of Tetraorganoborates and Related Group 13 Nucleophiles with Alkyl Halides. *Organometallics* **2014**, *33*, 5767−5780.

(22) Crockett, M. P.; Tyrol, C. C.; Wong, A. S.; Li, B.; Byers, J. A. Iron-Catalyzed Suzuki−Miyaura Cross-Coupling Reactions between Alkyl Halides and Unactivated Arylboronic Esters. *Org. Lett.* **2018**, *20*, 5233−5237.

(23) Bedford, R. B.; Nakamura, M.; Gower, N. J.; Haddow, M. F.; Hall, M. A.; Huwe, M.; Hashimoto, T.; Okopie, R. A. Iron-catalysed Suzuki coupling? A cautionary tale. *Tetrahedron Lett.* **2009**, *50*, 6110−6111.

(24) Tailor, S. B.; Manzotti, M.; Asghar, S.; Rowsell, B. J. S.; Luckham, S. L. J.; Sparkes, H. A.; Bedford, R. B. Revisiting Claims of the Iron-, Cobalt-, Nickel-, and Copper-Catalyzed Suzuki Biaryl Cross-Coupling of Aryl Halides with Aryl Boronic Acids. *Organometallics* **2019**, *38*, 1770−1777.

(25) Tailor, S. B.; Bedford, R. B. Can Immobilization of an Inactive Iron Species Switch on Catalytic Activity in the Suzuki Reaction? *Catal. Lett.* **2020**, *150*, 963−968.

(26) Bedford, R. B.; Gallagher, T.; Pye, D. R.; Savage, W. Towards iron-catalysed Suzuki biaryl cross-coupling: unusual reactivity of 2-halobenzyl halides. *Synthesis* **2015**, *47*, 1761−1765.
(27) O'Brien, H. M.; Manzotti, M.; Abrams, R. D.; Elorriaga, D.; Sparkes, H. A.; Davis, S. A.; Bedford, R. B. Iron-catalysed substrate-directed Suzuki biaryl cross-coupling. *Nat. Catal.* **2018**, *1*, 429−437.
(28) Neely, J. M.; Bezdek, M. J.; Chirik, P. J. Insight into transmetalation enables cobalt-catalyzed Suzuki−Miyaura cross coupling. *ACS Cent. Sci.* **2016**, *2*, 935−942.
(29) Asghar, S.; Tailor, S. B.; Elorriaga, D.; Bedford, R. B. Cobalt-catalyzed Suzuki biaryl coupling of aryl halides. *Angew. Chem., Int. Ed.* **2017**, *56*, 16367−16370.
(30) Duong, H. A.; Wu, W.; Teo, Y.-Y. Cobalt-catalyzed cross-coupling reactions of arylboronic esters and aryl halides. *Organometallics* **2017**, *36*, 4363−4366.
(31) Duong, H. A.; Yeow, Z.-H.; Tiong, Y.-L.; Kamal, N. H. B. M.; Wu, W. Cobalt-Catalyzed Cross-Coupling Reactions of Aryl Triflates and Lithium Arylborates. *J. Org. Chem.* **2019**, *84*, 12686−12691.
(32) Dunsford, J. J.; Clark, E. R.; Ingleson, M. J. Highly nucleophilic dipropanolamine chelated boron reagents for aryl-transmetallation to iron complexes. *Dalton Trans.* **2015**, *44*, 20577−20583.
(33) Hashimoto, T.; Gálvez, A. O.; Maruoka, K. In Situ Assembled Boronate Ester Assisted Chiral Carboxylic Acid Catalyzed Asymmetric Trans-Aziridinations. *J. Am. Chem. Soc.* **2013**, *135*, 17667−17670.
(34) Breunig, J. M.; Lehmann, F.; Bolte, M.; Lerner, H.-W.; Wagner, M. Synthesis and Reactivity of o-Phosphane Oxide Substituted Aryl(hydro)borates and Aryl(hydro)boranes. *Organometallics* **2014**, *33*, 3163−3172.
(35) Yu, D.-G.; Shi, Z.-J. Mutual Activation: Suzuki−Miyaura Coupling through Direct Cleavage of the sp^2 C-O Bond of Naphtholate. *Angew. Chem., Int. Ed.* **2011**, *50*, 7097−7100.
(36) Anson, C. E.; Klopper, W.; Li, J.-S.; Ponikiewski, L.; Rothenberger, A. A Close Look at Short C-CH_3···Potassium Contacts: Synthetic and Theoretical Investigations of $[M_2Co_2(\mu^3\text{-}O^tBu)_2(\mu^2\text{-}O^tBu)_4(thf)_n]$(M = Na, K, Rb, thf = tetrahydrofuran). *Chem. - Eur. J.* **2006**, *12*, 2032−2038.
(37) Brog, J.-P.; Crochet, A.; Seydoux, J.; Clift, M. J. D.; Baichette, B.; Maharajan, S.; Barosova, H.; Brodard, P.; Spodaryk, M.; Züttel, A.; Rothen-Rutishauser, B.; Kwon, N. H.; Fromm, K. M. Characteristics and properties of nano-$LiCoO_2$ synthesized by pre-organized single source precursors: Li-ion diffusivity, electrochemistry and biological assessment. *J. Nanobiotechnol.* **2017**, *15*, No. 58.
(38) Meyer, F.; Hempelmann, R.; Mathurb, S.; Veith, M. Microemulsion mediated sol−gel synthesis of nano-scaled MAl_2O_4 (M=Co, Ni, Cu) spinels from single-source heterobimetallic alkoxide precursors. *J. Mater. Chem.* **1999**, *9*, 1755−1763.
(39) Pauls, J.; Iravani, E.; Köhl, P.; Neumüller, B. Metalat Ions $[Al(OR)_4]^-$ as Chelating Ligands for Transition Metal Cations. *Z. Anorg. Allg. Chem.* **2004**, *630*, 876−884.
(40) Olmstead, M. M.; Power, P. P.; Sigel, G. Mononuclear cobalt(II) complexes having alkoxide and amide ligands: synthesis and x-ray crystal structures of $[Co(Cl)(OC\text{-}tert\text{-}Bu_3)_2.Li(THF)_3]$, $[Li(THF)_{4.5}][Co\{N(SiMe_3)_2\}(OC\text{-}tert\text{-}Bu_3)_2]$, and $[Li\{Co(N(SiMe_3)_2)(OC\text{-}tert\text{-}Bu_3)_2\}]$. *Inorg. Chem.* **1986**, *25*, 1027−1033.
(41) Bellow, J. A.; Fang, D.; Kovacevic, N.; Martin, P. D.; Shearer, J.; Cisneros, G. A.; Groysman, S. Novel Alkoxide Cluster Topologies Featuring Rare Seesaw Geometry at Transition Metal Centers. *Chem. - Eur. J.* **2013**, *19*, 12225−12228.
(42) Adams, C. J.; Bedford, R. B.; Carter, E.; Gower, N. J.; Haddow, M. F.; Harvey, J. N.; Huwe, M.; A'ngeles Cartes, M.; Mansell, S. M.; Mendoza, C.; Murphy, D. M.; Neeve, E. C.; Nunn, J. Iron(I) in Negishi Cross-Coupling Reactions. *J. Am. Chem. Soc.* **2012**, *134*, 10333−10336.
(43) Burés, J. A Simple Graphical Method to Determine the Order in Catalyst. *Angew. Chem., Int. Ed.* **2016**, *55*, 2028−2031.
(44) Lando, V. R.; Monteiro, A. L. Simple and Efficient Protocol for the Synthesis of Functionalized Styrenes from 1,2-Dibromoethane and Arylboronic Acids. *Org. Lett.* **2003**, *5*, 2891−2894.
(45) Moreno-Mañas, M.; Pérez, M.; Pleixats, R. Palladium-Catalyzed Suzuki-Type Self-Coupling of Arylboronic Acids. A Mechanistic Study. *J. Org. Chem.* **1996**, *61*, 2346−2351.
(46) Creary, X.; Mehrsheikh-Mohammadi, M. E.; McDonald, S. Methylenecyclopropane rearrangement as a probe for free radical substituent effects. *σ*. Values for commonly encountered conjugating and organometallic groups. *J. Org. Chem.* **1987**, *52*, 3254−3263.
(47) Neese, F. The ORCA program system. *Wiley Interdiscip. Rev.: Comput. Mol. Sci.* **2012**, *2*, 73−78.
(48) Neese, F. Software update: the ORCA program system, version 4.0. *Wiley Interdiscip. Rev.: Comput. Mol. Sci.* **2017**, *8*, No. e1327.
(49) Becke, A. D. Density-functional thermochemistry. III. The role of exact exchange. *J. Chem. Phys.* **1993**, *98*, 5648−5652.
(50) Lee, C.; Yang, W.; Parr, R. G. Development of the Colle-Salvetti correlation-energy formula into a functional of the electron density. *Phys. Rev. B* **1988**, *37*, 785−789.
(51) Vosko, S. H.; Wilk, L.; Nusair, M. Accurate spin-dependent electron liquid correlation energies for local spin density calculations: a critical analysis. *Can. J. Phys.* **1980**, *58*, 1200−1211.
(52) Stephens, P. J.; Devlin, F. J.; Chabalowski, C. F.; Frisch, M. J. Ab Initio Calculation of Vibrational Absorption and Circular Dichroism Spectra Using Density Functional Force Fields. *J. Phys. Chem. A* **1994**, *98*, 11623−11627.
(53) Grimme, S.; Ehrlich, S.; Goerigk, L. Effect of the damping function in dispersion corrected density functional theory. *J. Comput. Chem.* **2011**, *32*, 1456−1465.
(54) Neese, F.; Wennmohs, F.; Hansen, A.; Becker, U. Efficient, approximate and parallel Hartree-Fock and hybrid DFT calculations. A 'chain-of-spheres' algorithm for the Hartree−Fock exchange. *Chem. Phys.* **2009**, *356*, 98−109.
(55) Barone, V.; Cossi, M. Quantum Calculation of Molecular Energies and Energy Gradients in Solution by a Conductor Solvent Model. *J. Phys. Chem. A* **1998**, *102*, 1995−2001.
(56) Kozuch, S.; Shaik, S. How to Conceptualize Catalytic Cycles? The Energetic Span Model. *Acc. Chem. Res.* **2011**, *44*, 101−110.

https://dx.doi.org/10.1021/acscatal.0c05557
ACS Catal. 2021, 11, 3856−3866